Published in final edited form as:
Mol Cancer Res. 2014 December ; 12(12): 1704–1716. doi:10.1158/1541-7786.MCR-14-0291-T.

Restoration of Compact Golgi Morphology in Advanced Prostate Cancer Enhances Susceptibility to Galectin-1-induced Apoptosis by Modifying Mucin O-glycan Synthesis

Armen Petrosyan[1,2], **Melissa S. Holzapfel**[3], **David E. Muirhead**[3], and **Pi-Wan Cheng**[1,2,4]

[1]Nebraska Western Iowa Health Care System, Veteran Affairs Research Service, Omaha, NE

[2]Department of Biochemistry and Molecular Biology, College of Medicine, University of Nebraska Medical Center, Omaha, NE, USA

[3]Department of Pathology & Microbiology, University of Nebraska Medical Center, Omaha, NE, USA

[4]Eppley Institute for Research in Cancer and Allied Diseases, University of Nebraska Medical Center, Omaha, NE, USA

Abstract

Prostate cancer progression is associated with up-regulation of sialyl-T antigen produced by β-galactoside α-2,3-sialyltransferase-1 (ST3Gal1) but not with core 2-associated polylactosamine despite expression of core 2 N-acetylglucosaminyltransferase-L (C2GnT-L/*GCNT1*). This property allows androgen-refractory prostate cancer cells to evade galectin-1 (*LGALS1*)-induced apoptosis, but the mechanism is not known. We have recently reported that Golgi targeting of glycosyltransferases is mediated by golgins: giantin (*GOLGB1*) for C2GnT-M (*GCNT3*) and GM130 (*GOLGA2*)-GRASP65 (*GORASP1*) or GM130-giantin for core 1 synthase. Here, we show that for Golgi targeting, C2GnT-L also uses giantin exclusively while ST3Gal1 employs either giantin or GM130-GRASP65. In addition, the compact Golgi morphology is detected in both androgen-sensitive prostate cancer and normal prostate cells, but fragmented Golgi and mislocalization of C2GnT-L are found in androgen-refractory cells as well as primary prostate tumors (Gleason grade 2–4). Furthermore, failure of giantin monomers to be phosphorylated and dimerized prevents Golgi from forming compact morphology and C2GnT-L from targeting the Golgi. On the other hand, ST3Gal1 reaches the Golgi by an alternate site, GM130-GRASP65. Interestingly, inhibition or knockdown of non-muscle myosin IIA (*MYH9*) motor protein frees up Rab6a GTPase to promote phosphorylation of giantin by polo-like kinase 3 (PLK3), which is followed by dimerization of giantin assisted by protein disulfide isomerase A3 (PDIA3), and restoration of compact Golgi morphology and targeting of C2GnT-L. Finally, the Golgi relocation of C2GnT-L in androgen-refractory cells results in their increased susceptibility to galectin-1-induced apoptosis by replacing sialyl-T antigen with polylactosamine.

Corresponding author: Dr. Pi-Wan Cheng, Department of Biochemistry and Molecular Biology, University of Nebraska Medical Center, 985870 Nebraska Medical Center, Omaha, NE 68198-5870, USA. Phone: 402 559-5776. pcheng@unmc.edu.

The authors declare no competing financial interests.

Keywords

glycosyltransferases; Golgi fragmentation; giantin; non-muscle Myosin IIA; galectin-1-induced apoptosis

Introduction

Prostate cancer, the second leading cause of cancer-related death in men around the world (1), has been shown to produce altered O-glycans and galectins (2, 3). Among the commonly used prostate cancer cells, LNCaP cells are androgen-sensitive while PC-3 and DU145 cells are androgen-refractory and more aggressive than LNCaP cells (4). Interestingly, PSA (+) LNCaP cells, which express high level of core 2 N-acetylglucosaminyltransferase-L (C2GnT-L/*GCNT1*), produce polylactosamine and are susceptible to galectin-1-induced apoptosis (5). However, PC-3 and DU145 cells do not synthesize polylactosamine and are resistant to galectin-1 despite expression of both C2GnT-L and β-galactoside α-2,3-sialyltransferase-1 (ST3Gal1)(Fig. 1A) (6). The mechanism is not known.

During cancer development and progression, aberrant O-glycans (7), including sialylated Lewis and Thomsen-Friedenreich (T) antigens (8), are frequently reported. Altered expression of certain glycosyltransferase (GT) genes involved in the synthesis of these tumors-associated carbohydrates has been proposed. For example, upregulation of C2GnT-L produces core 2 structure, Galβ1-3(GlcNAcβ1-6)GalNAc, from core 1 or T-antigen, Galβ1-3GalNAc (Fig. 1A), to allow decoration with polylactosamine or sialyl Lewis antigens at the non-reducing termini (9). Down-regulation of same enzyme results in production of elevated sialyl-T antigen, Siaα2-3Galβ1-3GalNAc, which is formed by ST3Gal1 (Fig. 1A). Because the core 1 structure formed by Core 1 synthase (C1GalT1) is the substrate for both C2GnT-L and ST3Gal1, and C2GnT-L and ST3Gal1 are localized to *cis-medial-* and *medial-trans*-Golgi, respectively (10, 11), the core 2 structure is preferentially generated in the presence of C2GnT-L, while sialyl-T antigen is abundantly formed when C2GnT-L is missing. However, the dominance ofST3Gal1-directed O-glycosylation pathway over the C2GnT-L-directed branching in the advanced prostate cancer cells cannot be attributed to the lack of expression of *C2GnT-L* gene, *GCNT1* (6, 11,12). The failure of C2GnT-L to target the Golgi of these cells may be a possible explanation.

The Golgi apparatusis a dynamic posttranslational modification and sorting station for secreted and membrane-bound proteins. It undergoes constant remodeling under normal physiological conditions and significant morphological changes in response to stress. Further, Golgi fragmentation and altered glycosylation have been reported in prostate cancer (13), but the significance of their link is only beginning to be understood (14, 15). Recently, we (16) and others (17, 18) have shown that Golgi residential GTs are retained in the Golgi by binding via the cytoplasmic tails to their cognate proteins. In addition to participation in the retention of GTs, the cytoplasmic tails of Golgi GTs also bind directly, specifically, and tightly to a motor protein, non-muscle myosin IIA (NMIIA/*MYH9*) to mediate normal

recycling of the Golgi GTs and Golgi fragmentation (19, 20). Inhibition or knockdown (KD) of NMIIA blocks Golgi remodeling and reverses the fragmented Golgi to compact morphology (15). In this communication, we show that ST3Gal1 uses GM130-GRASP65 and giantin while C2GnT-L utilizes only giantin for Golgi targeting. We also discover that defective giantin dimerization in PC-3 and DU145 cells causes fragmentation of the Golgi and prevents C2GnT-L but not C1GalT1 and ST3Gal1 from targeting the Golgi. Finally, we find that reformation of the compact Golgi morphology in advanced prostate cancer cells also restores Golgi targeting of C2GnT-L, which results in the synthesis of polylactosamine and renders these cells susceptible to galectin-1-induced apoptosis.

Materials and methods

Antibodies

The primary antibodies were: a) rabbit polyclonal – NMIIA (Sigma, M8064), giantin (ab24586), PDIA3 (ab13507), Plk3 (ab67922) and Rab6a (ab95954) (Abcam), GRASP65 and AR (androgen receptor) (Santa Cruz Biotechnology, sc-30093 and sc-816, respectively); b) rabbit monoclonal – GM130 (Abcam, ab52649); c) mouse monoclonal – C1GalT1 and Rab6a (Abcam, ab57492 and ab55660, respectively), β-actin (Sigma, A2228), GRASP65 (Santa Cruz Biotechnology, sc-365434), giantin (Abcam, ab37266); d) mouse polyclonal – C2GnT-L and ST3Gal1 (Abnova, H00002650-B01P and H00006482-B01P, respectively). The secondary antibodies (Jackson ImmunoResearch) were: a) HRP-conjugated donkey anti-rabbit and donkey anti-mouse for Western-blotting (W-B) (711-035-152 and 715-035-151, respectively); b) donkey anti-mouse Alexa Fluor 488 and anti-rabbit Alexa Fluor 594 (115-546-003 and 711-585-152, respectively) and DyLight 594-conjugated monoclonal mouse anti-biotin for immunofluorescence (IF) (200-512-211).

Cell culture and drug treatment

LNCaP cells are provided by Dr. Ming-Fong Lin, and PC-3 and DU145 cells obtained from the Americal Type Culture were grown as described previously (15). Blebbistatin (Sigma) was dissolved in dimethyl sulfoxide (DMSO) immediately before use. Cells treated with a corresponding concentration of DMSO served as controls. The regular working concentration for Blebbistatin was 25 μM and treatment time for up to 16 h.

Co-immunoprecipitation (CO-IP) and transfection

Co-IP assay was performed on cell lysate using Pierce Co-Immunoprecipitation Kit (Pierce) according to manufacturer's instructions. *MYH9* (myosin, heavy polypeptide 9, non-muscle), *GOLGB1* (giantin), *GOLGA2* (GM130), *GORASP1* (GRASP65), *Rab6a*, *PDIA3*, *Plk3*, *AR* and scrambled on-targetplussmartpool siRNAs were purchased from Santa Cruz Biotechnology and Dharmacon. All products were consisted of pools of three to five target-specific siRNAs. Cells were transfected with 100–200 nM siRNAs using LipofectamineRNAi MAX reagent (Life science technologies). Full length human PDIA3 cDNA in pGEc2-DEST (Flag-tagged mammalian expression vector) was obtained from DNASU Plasmid Repository. Transient transfection of LNCaP cells was carried out using the Lipofectamine 2000 (Life Science technologies) following the manufacturer's protocol.

Proteins were separated on SDS PAGE on mini-gels with various % gel specified for each experiment (Bio-Rad).

Confocal immunofluorescence microscopy and isolation of Golgi membrane fractions by sucrose gradient centrifugation were performed as described previously (15). Normal human prostate and prostate adenocarcinoma tissue arrays were purchased from US Biomax. For lectins staining, the cells were incubated for 15 min at RT with 1.7 μM streptavidin (Sigma) diluted in PBST. After washing, cells were treated for 1 h at RT by 2 mM biotin (Sigma) dissolved in PBST followed by washing 3× with PBST and incubation for 3 h at RT with 10 μg/ml of biotinylated lectins (EY Laboratories). After washing, cells were incubated for another 1 h at RT with DyLight594 anti-biotin Abs. The average fluorescence intensity was measured as a mean ± SEM of integrated fluorescence intensity (in arbitrary units, a.u.) or total fluorescence intensity (in pixels) measured for every cell individually. The Golgi region (perinuclear area) and cytoplasm (ER) regions were determined using the intensity of the Golgi markers (giantin, GM130 or GRASP65) and ER marker (HSP70) staining. Nuclei were counterstained with DAPI (blue). Statistical analysis of colocalization was performed by ImageJ calculating the Mander's overlap coefficient, corresponding to the fraction of green pixels that overlap with red pixels relative to the total green pixels (21).

Lectin-binding assay

IP samples were diluted with cell lysis buffer and incubated with 100 μl of SNA- and PSL-containing agarose beads or 100 μg of biotinylated Con A lectin (EY Laboratories) overnight at 4°C with end-over-end mixing. Con A-specific sample was incubated additionally with 50 μl of Dynabeads M-280 streptavidin (Dynal) for 30 min at RT followed by immobilization with a magnet. All magnet-isolated samples were analyzed by SDS PAGE and probed with anti-giantin Ab.

Transmission Electron Microscopy

All specimens were processed using Leica AMW Microwave processing technology. Specimens were fixed in Trumps fixative (American Master Tech) and embedded in HistoGel (Thermo Scientific) then post-fixed in 1% Osmium Tetroxide. The fixed cell pellets were washed and dehydrated using a graded acetone series and infiltrated with PolyBed 812 epoxy resin. 0.1 micron thick sections were stained with 1% Toluidine blue and examined under the light microscope. Selected areas were ultrasectioned (70–90 nm, Silver sections), mounted on copper grids and stained with uranyl acetate and lead citrate. Sections were screened on a JEOL 1230 transmission electron microscope at 60KV and imaged using a Keen View bottom mount camera and ITEM Soft Imaging Solutions Digital Software and representative electron micrographs taken.

Phosphorylation and the plasma membrane protein isolation assay

Cell samples were resuspended in EDTA-free CIP buffer, containing 100 mM NaCl, 50 mM Tris-HCl, 10 mM $MgCl_2$, and 1 mM DTT (New England Biolabs). Cell lysates were further treated with CIP (New England Biolabs) (1 unit CIP per microgram of protein) in the absence or presence of a phosphatase inhibitor, β-glycerophosphate (50 mM) for 60 min at 37°C. Then, samples were analyzed by SDS PAGE followed by W-B. Cell surface proteins

were isolated with a Pierce Chemical kit, and incubated overnight at 4°C with biotinylated lectins. Next, samples were pulled down by Dynabeads M-280 streptavidin for 30 min at RT followed by immobilization with a magnet. Obtained samples were analyzed by 8% SDS PAGE. Densitometric analysis of band intensity was performed using ImageJ.

RT-PCR analysis of gene expression

RNA from cultured prostate cells was isolated by TRI-REAGENT (MRC Inc.) according to the manufacturer's instruction. To prepare cDNA, 2 μg RNA was used in a 20 μl reaction mixture using a Verso reverse transcriptase kit (Thermo scientific) as follows: 5 min at RT, 60 min at 42°C, and 2 min at 95°C. Quantitative real-time PCR was performed in 10 μl reaction volume in a 96-well plate using 2 μl of diluted (1:1) cDNA with SYBR® Premix Ex Taq™ (Takar Bio Inc.) on a Mastercycler Epgradient realplex (Eppendorf). The PCR conditions included 1 cycle at 95°C for 2 min followed by 45cycles at 95°C for 15 s, 60°C for 15 s, and 72°C for 45 s. The data were analyzed using Eppendorf realplex software, version 1.5 (Eppendorf). Glyceraldehyde-3-phosphate dehydrogenase (GAPDH) was included for every sample as the control reaction. Relative fold differences in transcript expression were determined using the following comparative CT method: $2^{-[\Delta Ct\ (Target)]}\times 100$ where $\Delta Ct = Ct(Target) - Ct\ (GAPDH)$ as described previously (22). The results were expressed as the fold relative to that (100 %, 1 fold) of GAPDH.

Galectin-1 prostate cell apoptosis assays

Cells cultured in 6-well plates and in T-75 flasks were treated with 10μM galectin-1 (Abcam) in 1.2 mM DTT for 7 h at 37°C. The supernatant was removed and adherent cells on coverslips were rinsed with PBS and counter-stained with DAPI Mounting. Apoptotic nuclei were then visualized under a fluorescence microscope. For measuring caspase-3 activity, cells were collected with a plastic scraper, resuspended by gentle pipetting in PBS followed by protocol according to Millipore's caspase-3 colorimetric activity assay kits. Fluorescence was measured at excitation at 400 nm and emission at 505 nm.

Miscellaneous

Protein concentrations were determined with the Coomassie Plus Protein Assay (Pierce Chemical Co). The results shown are representative of three independent experiments. Data are expressed as mean ± SEM. Analysis was performed using 2-sided t-test. A value of $P < 0.05$ was considered statistically significant.

Results and Discussion

Differential Golgi targeting of ST3Gal1 and C2GnT-L in androgen-refractory prostate cancer cells and adenocarcinoma tumors

We found that in PSA (+) LNCaP cells (hereafter LNCaP), Golgi appeared as a compact morphology and localized in juxtanuclear area, while heterogeneous size Golgi fragments were detected in PC-3 and DU145 cells (Fig. 1B). Next, we screened the Golgi localization of three key early O-glycosylation enzymes, C1GalT1, ST3Gal1 and C2GnT-L. In LNCaP cells, all three GTs were found in the Golgi but not in the ER as determined by co-staining with Golgi marker, giantin (*GOLGB1*), and an endoplasmic reticulum (ER) marker, HSP70

(Fig. 1B and C, and Supplementary Fig. S1A). But, in PC-3 and DU145 cells, C1GalT1 and ST3Gal1 were detected in the Golgi while C2GnT-L in the ER (Fig. 1B and C, and Supplementary Fig. S1A). The intra-Golgi localization of C1GalT1 and ST3Gal1 as well as ER-specific distribution of C2GnT-L in PC-3 and DU145 cells was further confirmed by co-staining of these GTs with other Golgi markers, GM130 (*GOLGA2*) and Golgi-specific GTPase Rab6a (Supplementary Fig. S2A, B). Predictably, all three GTs were in the compact Golgi of normal prostate cells (Fig. 1D). Like the androgen-refractory prostate cancer cells, the adenocarcinoma cells of Gleason grade 2–4 prostate tumors also exhibit fragmented Golgi, which ranged from disorganized to multiple fragments at Gleason grades 2 and 3 to extensively dispersed at grade 4. Further, the distribution of these enzymes was asymmetric, with C1GalT1 and ST3Gal1 in the Golgi, and C2GnT-L in the ER (Fig. 1D, E, and Supplementary Fig. S1B). The data indicate that the altered Golgi morphology and mislocalization of C2GnT-L in PC-3 and DU145 cells resemble those found in the adenocarcinoma cells of prostate tumors, suggesting that these two cell lines could serve as *in vitro* cell models for elucidating the mechanism of Golgi fragmentation and C2GnT-L mislocalization in prostate tumors.

In a recent report, we have demonstrated that two GTs utilize different Golgi matrix proteins (golgins) for Golgi targeting: C1GalT1 uses GM130-GRASP65 (*GORASP1*) or GM130-giantin, while core 2 N-acetylglucosaminyltransferase-M (C2GnT-M/*GCNT3*), anisozyme of C2GnT-L, employs giantin exclusively (23). In light of this, we monitored the Golgi localization of ST3Gal1 in LNCaP cells after siRNA KD of different golgins. In cells lacking giantin, GM130 or GRASP65, ST3Gal1 was still in the Golgi (Fig. 2A,C,D). In giantin plus GM130 double-KD cells, ST3Gal1 was in the cytoplasm instead of the Golgi as shown by immunostaining of Rab6a, suggesting that both GM130-GRASP65 complex and giantin are the Golgi docking sites for ST3Gal1 (Fig. 2A,C,E). The failure of C2GnT-L to reach the Golgi of LNCaP cells after KD of giantin confirms the exclusive requirement of giantin for Golgi targeting of C2GnT-L (Fig. 2A,C,D,E) (23). As predicted, in LNCaP cells, Golgi targeting of C1GalT1 is mediated by GM130 (Fig. 2B,C), and KD of GRASP65 did not affect the protein level of its partner, GM130, because in the absence of GRASP65, GM130 is still retained in the Golgi through interaction with giantin, as previously described (23, 24), thereby serving as an alternative docking site for C1GalT1 (Fig. 2E, blue box and 2F). Surprisingly, the same phenomenon was not detected in PC-3 and DU145 cells. Quite contrary, KD of GRASP65 significantly reduced level of GM130 (Fig. 2F) and had no effect on GM130 gene expression (Fig. 2G), suggesting that GM130 was unable to function without GRASP65 due to unavailability of the other partner, giantin. Indeed, in PC-3 and DU145 cells, C1GalT1 was detected outside of the Golgi after KD of either GRASP65 or GM130 (Supplementary Fig. S3A–D). Further, this conclusion was confirmed by failure of ST3Gal1 to reach the Golgi after KD of GM130 in PC-3 and DU145 cells (Fig. 2A,C). Taken together, these data suggest that in androgen-refractory prostate cancer cells, altered function/structure of giantin renders C2GnT-L unable to target the Golgi while C1GalT1 and ST3Gal1 utilizes GM130-GRASP65 as an alternate Golgi targeting site in the absence of functional giantin (Fig. 2H). The two key questions that need to be answered include the nature of the giantin defect in PC-3 and DU145 cells, and how the defect affects the Golgi morphology and targeting of C2GnT-L.

Characterization of the giantin in PC-3 and DU145 cells

Golgins, including GM130, GRASP65, and p115, are known to participate in the maintenance of Golgi morphology and biogenesis after Golgi disassembly (25–27). However, very little is known about the involvement of giantin in these processes despite the fact that giantin is essential for cross-bridging cisternae during Golgi biogenesis (28) and more stably associated with Golgi fragments than other golgins during apoptosis (29, 30). Giantin is the highest molecular weight (376 kDa) Golgi matrix protein. It consists of a short C-terminal domain located in the Golgi lumen (31), where a disulfide bond connects two monomers to form an active homodimer, which is followed by a one-pass transmembrane domain and then a large (≥350 kDa) N-terminal region (28, 32).

To investigate the function of giantin, we analyzed its dimerization in all three prostate cancer cells. We detected the giantin dimer in LNCaP cells, but not PC-3 and DU145 cells under standard SDS PAGE condition, i.e. in the presence of 5% β-mercaptoethanol (β-ME) (Fig. 3A–C). By lowering β-ME level from 5% to 1%, more giantin dimer was detected in LNCaP cells, confirming that the dimer is formed by disulfide bond (28) (Fig. 3A). It was also noted that the giantin monomer in LNCaP cells exhibited slower mobility than that in PC-3 and DU145 cells (Fig. 3B,C), raising the possibility that the giantin monomer in LNCaP cells but not PC-3 and DU145 cells was posttranslationallly modified, such as phosphorylation. As shown in Fig. 3D, the giantin monomer band after treatment of LNCaP cells lysate with calf intestinal alkaline phosphatase (CIP) exhibited same mobility as that in PC-3 and DU145 cells. The phosphatase-specific action was abolished after treatment with a general phosphatase inhibitor, β-glycerophosphate (β-GP). The result indicates that the giantin monomer in LNCaP but not the other two prostate cancer cells is phosphorylated.

Protein disulfide isomerase A3 (PDIA3) and Rab6a are involved in dimerization of giantin

We examined the possible involvement of a glycoprotein-specific disulfide isomerase (PDIA3) (33) in giantin dimerization because giantin is a glycoprotein (Fig. 3E) and PDIA3 is down-regulated in aggressive prostate cancer cells and tumors (34). In recent years, it has become clear that PDI enzymes function in not only the ER but also ER-Golgi intermediate, ERGIC (35), and on the cell surface (36). Interestingly, in LNCaP cells, the level of PDIA3 protein was substantially higher than that in PC-3 and DU145 cells (Fig. 3F), and PDIA3 IF staining signal was detected in the Golgi area (Fig. 3G). To gain a better understanding of the degree of giantin and PDIA3 interaction in these cells, a bidirectional Co-IP was employed. We detected a higher degree of association of giantin and PDIA3 in LNCaP cells than that in PC-3 and DU145 cells (Fig. 3H,I). The result was reproduced using the Golgi fractions of these three cells (Fig. 3J), confirming that the interaction occurs at the Golgi. Further, KD of PDIA3 in LNCaP cells caused Golgi fragmentation and reduced giantin and C2GnT-L without affecting GM130 (Fig. 3G,K,L). Significantly, siRNA silencing of PDIA3 did not change the expression of neither giantin nor C2GnT-L gene (Fig. 3M) but resulted in a decrease of both phosphorylated and dimerized giantin (Fig. 3N). The data suggest that defective giantin in PC-3 and DU145 cells undergoes proteasomal degradation (24). Finally, the level of giantin protein in LNCaP cells was elevated after transfection with PDIA3 cDNA (Fig. 3O), which further confirms the close association of giantin with PDIA3.

Next, we examined the possible involvement of Rab6a GTPase in the NMIIA-mediated Golgi fragmentation and the giantin-involved maintenance of Golgi morphology. It is known that GTPase activity of Rab6a protein is essential for its interaction with NMIIA (37) and giantin (38). Rab6a regulates the intra-Golgi localization of NMIIA and facilitates the action of protein kinases (37, 39). KD of Rab6a significantly changes the Golgi morphology from a classical perinuclear compact shape to fragmented, collapsed or expanded structures (40, 41). We detected Rab6a-giantin complex prominently in LNCaP, but not PC-3 and DU145 cells (Fig. 4A). Further, we found that in cells lacking Rab6a, Golgi was fragmented, and this disorganization was accompanied by reduced amounts of giantin, including total, dimer and phosphorylated monomer (Fig. 4B–D). Notably, the Rab6a siRNA treatment did not affect the expression of giantin gene (Fig. 4E).

Because LNCaP cells, but not PC-3 and DU145, produce abundant amounts of androgen receptor (AR) (Fig. 4F), and several androgen-responsive molecules in the Golgi are considered to be important for both prostate cancer development and treatment (42–44), we analyzed whether AR regulates Golgi morphology. We found that treatment of LNCaP cells with AR siRNA did not alter the Golgi morphology (Fig. 4G,H). Moreover, the amounts of giantin, C2GnT-L, ST3Gal1 or C1GalT1 proteins were unaffected and cells exhibited Golgi-specific staining patterns for these GTs (Fig. 4G,H). Therefore, the defective giantin structure and consequent Golgi fragmentation in advanced prostate cancer cells cannot be ascribed to the down-regulation of AR.

Inhibition or KD of NMIIA restores compact Golgi morphology in PC-3 and DU145 cells by induction of giantin dimerization through giantin phosphorylation by Polo-like kinase 3

In agreement with our previous observation in colon cancer cells (15), here we found that inhibition of NMIIA with Blebbistatin (Blebb) or treatment with NMIIA siRNAs in PC-3 and DU145 cells also restored the compact Golgi morphology (Fig. 5A–C, Supplementary Fig. S4A), as measured by the number of Golgi fragments (Fig. 5C). Notably, we observed that inhibition of NMIIA resulted in an increase of giantin and PDIA3 (Fig. 5D), and dissociation of Rab6a from NMIIA (Fig. 5E) and association of PDIA3 with giantin (Fig. 5F). Most significantly, C2GnT-L was relocated to the Golgi, as detected by Mander's overlap coefficient between C2GnT-L and giantin (Fig. 5A,G). Further, the NMIIA dysfunction/deficiency was accompanied by phosphorylation of giantin (Fig. 5H,I).

The phosphorylation of giantin under mitotic conditions has been shown both *in vitro* and *in vivo* (45). In search of giantin-specific kinase, we focused on Polo-like kinase 3 (Plk3) because it is widely present in the Golgi and associated with giantin (46). We found that in LNCaP cells, KD of Plk3 caused a decrease of giantin phosphorylation and dimerization, and resulted in Golgi fragmentation (Fig. 5J–L) but did not change the levels of giantin mRNA (Fig. 5M). Interestingly, the Plk3-giantin complex typically detected in control cells was substantially reduced after KD of Rab6a, indicating that interaction of Rab6a with giantin precedes its phosphorylation by Plk3 (Fig. 5N). Furthermore, depletion of Plk3 abolished the Golgi restoration effect of either Blebb or NMIIA KD suggesting that Golgi biogenesis in PC-3 and DU145 cells requires giantin phosphorylation by Plk3 (Fig. 5O, Supplementary Fig. S4B).

In summary, we found that inhibition or depletion of NMIIA in PC-3 and DU145 cells is sufficient to rescue normal Golgi morphology and return C2GnT-L to the Golgi. Not surprisingly, in high-grade prostate cancer cells, the Rab6a gene is up-regulated (47), and here we show that Rab6a tightly associates with NMIIA in the fragmented Golgi of advanced prostate cancer cells, which prevents its association with and activation of giantin. The data suggest that loss of NMIIA function reactivates giantin phosphorylation by Plk3, which facilitates its dimerization assisted by PDIA3, and in turn leads to the connection of the Golgi stacks (Fig. 6A).

The effect of NMIIA inhibition on Golgi ultrastructure was analyzed in detail by transmission electron microscopy (Fig. 6B). In LNCaP cells, the Golgi is localized in the perinuclear space, and is present as a monolithic structure consisted of a mix of dilated and flattened dictyosomes that are often expanded at their ends. We also observed prominent vesicular components which are mostly localized at the *trans*-face of the Golgi. The PC-3 and DU145 cells have an extensive Golgi with multiple stunted dictyosomes distributed across the cytoplasm which mostly appeared as few linear stacks clustered together (Fig. 6B, white arrows). Secretory activity is present as vesicles and vesicular membrane clusters distributed between the fragments of Golgi membranes (Fig. 6B, white arrowheads). Blebb treatment converted the Golgi in these two cells into a compact structure within the perinuclear area. Further, the Golgi dictyosomes became prolonged and dilated, and the vesicular elements were predominantly localized at the *trans*-Golgi.

Restoration of compact Golgi morphology in PC-3 and DU145 cells is accompanied by production of polylactosamine glycans and increases their susceptibility to galectin-1-induced apoptosis

As a result of restoring compact Golgi morphology and C2GnT-L Golgi targeting in both PC-3 and DU145 cells, the α-2,3-Sia structure revealed by MAA lectin (*Maackia amurensis* agglutinin) staining was greatly reduced, which was accompanied by an increase of polylactosamine structure as detected by LEA lectin (*Lycopersicon esculentum* agglutinin) staining (Fig. 7A–D, Supplementary Fig. S5A–D). Similar to the expression of MAA-specific proteins in the plasma membrane fractions was significantly reduced after treatment with Blebb or NMIIA siRNA, as determined by densitometry of the Coomassie stained gel. Meantime, LEA-specific signal was enriched (Fig. 7E, Supplementary Fig. S5E). Similarly to LNCaP cells (Fig. 7F), such increase of polylactosamine in PC-3 and DU145 cells also led to their enhanced susceptibility to cell death induced by galectin-1 (10 μM for 7h). Only minor internucleosome DNA degradation was observed in control cells treated with either DMSO or Blebb and either scramble or NMIIA siRNA as measured by DAPI staining. Meantime, treatment of PC-3 and DU145 cells with Blebb or NMIIA siRNA followed by incubation with galectin-1 induced significant internucleosome DNA degradation (Fig. 7G, H, Supplementary Fig. S5F,G). We also detected in these cells an8-fold increase in caspase-3 activity compared with the control (Fig. 7I, Supplementary Fig. S5H). These data confirm the phenomenon described by Valenzuela et al. (5) that galectin-1 induces apoptosis in androgen-sensitive and PSA (+) LNCaP prostate cancer cells (Fig. 7F), which produce polylactosamine, but not PSA (−) LNCaP and androgen-refractory PSA (−) DU145 cells, which are devoid of polylactosamine.

The detection of sialyl-T tumor antigen in PC-3 and DU145 cells is consistent with the report that this antigen is associated with tumor progression (8). One important message we have provided in this study is that the generation of sialyl-T antigen in these cells is not the consequence of down-expression of C2GnT-L, which is known to preempt the action of ST3Gal1, but rather the inability of C2GnT-L to target the Golgi. In support of this conclusion, we have shown that sialyl-T antigen ceases to be produced following the return of C2GnT-Lto the Golgi after inhibition or KD of NMIIA (Fig. 6C). Therefore, the level of expression of C2GnT-L alone cannot be used as a prognostic marker of prostate cancer progression (48), implying that Golgi localization of this enzyme is an important determinant. Another exciting finding is the functional consequence of C2GnT-L mislocalization which leads to the reduced production of core 2-associated polylactosamine. As a result, androgen-refractory prostate cancer cells acquire a survival advantage by evading apoptosis induced by galectin-1.

In summary, we provide a general model of giantin role for the biogenesis and maintenance of compact Golgi morphology and regulation of O-glycosylation. Moreover, we show that restoration of compact Golgi via blocking of NMIIA may be an effective mechanism to enhance tumor cell susceptibility to death induced by galectin-1. We believe this finding will help to open new perspectives for understanding the “oncological Golgi” and its role in cancer progression and metastasis.

Supplementary Material

Refer to Web version on PubMed Central for supplementary material.

Acknowledgments

Financial Support: This work is supported in part by the Office of Research and Development, Medical Research Service, Department of Veterans Affairs (VA 1I1BX000985), the NIH (1R21HL097238) and the State of Nebraska (LB506).

References

1. Siegel R, Naishadham D, Jemal A. Cancer statistics, 2013. CA Cancer J Clin. 2012; 63:11–30. [PubMed: 23335087]
2. Oka N, Takenaka Y, Raz A. Galectins and urological cancerz. J Cell Biochem. 2004; 91:118–124. [PubMed: 14689585]
3. Peracaula R, Tabarés G, Royle L, Harvey DJ, Dwek RA, Rudd PM, et al. Altered glycosylation pattern allows the distinction between prostate-specific antigen (PSA) from normal and tumor origins. Glycobiology. 2003; 13:457–470. [PubMed: 12626390]
4. Dozmorov MG, Hurst RE, Culkin DJ, Kropp BP, Frank MB, Osban J, et al. Unique patterns of molecular profiling between human prostate cancer LNCaP and PC-3 cells. Prostate. 2009; 69:1077–1090. [PubMed: 19343732]
5. Valenzuela HF, Pace KE, Cabrera PV, White R, Porvari K, Kaija H, et al. O-glycosylation regulates LNCaP prostate cancer cell susceptibility to apoptosis induced by galectin-1. Cancer Res. 2007; 67:6155–6162. [PubMed: 17616672]
6. Gao Y, Chachadi VB, Cheng PW, Brockhausen I. Glycosylation potential of human prostate cancer cell lines. Glycoconj J. 2012; 29:525–537. [PubMed: 22843320]
7. Varki, A.; Kannagi, R.; Toole, BP. Essentials of Glycobiology. 2nd edition. Vol. 44. New York: Cold Spring Harbor; 2009. Glycosylation Changes in Cancer; p. 617-633.

8. Dabelsteen E. Cell surface carbohydrates as prognostic markers in human carcinomas. J Pathol. 1996; 179:358–369. [PubMed: 8869281]
9. Ellies LG, Tsuboi S, Petryniak B, Lowe JB, Fukuda M, Marth JD. Core 2 oligosaccharide biosynthesis distinguishes between selectin ligands essential for leukocyte homing and inflammation. Immunity. 1998; 9:881–890. [PubMed: 9881978]
10. Whitehouse C, Burchell J, Gschmeissner S, Brockhausen I, Lloyd KO, Taylor-Papadimitriou J. A transfected sialyltransferases that is elevated in breast cancer and localizes to the medial/trans-Golgi apparatus inhibits the development of core-2-based O-glycans. J Cell Biol. 1997; 137:1229–1241. [PubMed: 9182658]
11. Dalziel M, Whitehouse C, McFarlane I, Brockhausen I, Gschmeissner S, Schwientek T. The relative activities of the C2GnT1 and ST3Gal-I glycosyltransferases determine O-glycan structure and expression of a tumor-associated epitope on MUC1. J Biol Chem. 2001; 276:11007–11015. [PubMed: 11118434]
12. Schneider F, Kemmner W, Haensch W, Franke G, Gretschel S, Karsten U, et al. Overexpression of sialyltransferase CMP-sialic acid: Galbeta1, 3GalNAc-R alpha6-Sialyltransferase is related to poor patient survival in human colorectal carcinomas. Cancer Res. 2001; 61:4605–4611. [PubMed: 11389097]
13. Mao P, Nakao K, Angrist A. Human prostatic carcinoma: an electron microscope study. Cancer Res. 1966; 26:955–973. [PubMed: 5934805]
14. Kellokumpu S, Sormunen R, Kellokumpu I. Abnormal glycosylation and altered Golgi structure in colorectal cancer: dependence on intra-Golgi pH. FEBS Lett. 2002; 516:217–224. [PubMed: 11959136]
15. Petrosyan A, Cheng PW. A non-enzymatic function of Golgi glycosyltransferases: mediation of Golgi fragmentation by interaction with non-muscle myosin IIA. Glycobiology. 2013; 23:690–708. [PubMed: 23396488]
16. Ali MF, Chachadi VB, Petrosyan A, Cheng PW. Golgi phosphoprotein 3 determines cell binding properties under dynamic flow by controlling Golgi localization of core 2 N-acetylglucosaminyltransferase 1. J Biol Chem. 2012; 287:39564–39577. [PubMed: 23027862]
17. Schmitz KR, Liu J, Li S, Setty TG, Wood CS, Burd CG, et al. Golgi localization of glycosyltransferases requires a Vps74p oligomer. Dev Cell. 2008; 14:523–534. [PubMed: 18410729]
18. Pereira NA, Pu HX, Goh H, Song Z. Golgi phosphoprotein 3 mediates the Golgi localization and function of protein O-linked mannose β-1,2-Nacetlyglucosaminyltransferase 1. J Biol Chem. 2014 Apr 14. (in press).
19. Petrosyan A, Ali MF, Verma SK, Cheng H, Cheng PW. Non-muscle myosin IIA transports a Golgi glycosyltransferase to the endoplasmic reticulum by binding to its cytoplasmic tail. Int J Biochem Cell Biol. 2012; 44:1153–1165. [PubMed: 22525330]
20. Petrosyan A, Cheng PW. Golgi fragmentation induced by heat shock or inhibition of heat shock proteins is mediated by non-muscle myosin IIA via its interaction with glycosyltransferases. Cell Stress Chaperones. 2013; 19:241–254. [PubMed: 23990450]
21. Comeau JW, Costantino S, Wiseman PW. A guide to accurate fluorescence microscopy colocalization measurements. Biophys J. 2006; 91:4611–4622. [PubMed: 17012312]
22. Tassone F, Hagerman RJ, Taylor AK, Gane LW, Godfrey TE, Hagerman PJ. Elevated levels of FMR1 mRNA in carrier males: a new mechanism of involvement in the fragile-X syndrome. Am J Hum Genet. 2000; 66:6–15. [PubMed: 10631132]
23. Petrosyan A, Ali MF, Cheng PW. Glycosyltransferase-specific Golgi-targeting mechanisms. J Biol Chem. 2012; 287:37621–37627. [PubMed: 22988244]
24. Puthenveedu MA, Bachert C, Puri S, Lanni F, Linstedt AD. GM130 and GRASP65-dependent lateral cisternal fusion allows uniform Golgi-enzyme distribution. Nat Cell Biol. 2006; 8:238–248. [PubMed: 16489344]
25. Dirac-Svejstrup AB, Shorter J, Waters MG, Warren G. Phosphorylation of the vesicle-tethering protein p115 by a casein kinase II-like enzyme is required for Golgi reassembly from isolated mitotic fragments. J Cell Biol. 2000; 150:475–488. [PubMed: 10931861]

26. Lin CY, Madsen ML, Yarm FR, Jang YJ, Liu X, Erikson RL. Peripheral Golgi protein GRASP65 is a target of mitotic polo-like kinase (Plk) and Cdc2. Proc Natl Acad Sci U S A. 2000; 97:12589–12594. [PubMed: 11050165]
27. Lowe M, Gonatas NK, Warren G. The mitotic phosphorylation cycle of the cis-Golgi matrix protein GM130. J Cell Biol. 2000; 149:341–356. [PubMed: 10769027]
28. Linstedt AD, Hauri HP. Giantin, a novel conserved Golgi membrane protein containing a cytoplasmic domain of at least 350 kDa. Mol Biol Cell. 1993; 4:679–693. [PubMed: 7691276]
29. Nozawa K, Casiano CA, Hamel JC, Molinaro C, Fritzler MJ, Chan EK. Fragmentation of Golgi complex and Golgi autoantigens during apoptosis and necrosis. Arthritis Res. 2002; 4:R3. [PubMed: 12106502]
30. Nozawa K, Fritzler MJ, von Mühlen CA, Chan EK. Giantin is the major Golgi autoantigen in human anti-Golgi complex sera. Arthritis Res Ther. 2004; 6:R95–R102. [PubMed: 15059272]
31. Sönnichsen B, Lowe M, Levine T, Jämsä E, Dirac-Svejstrup B, Warren G. A role for giantin in docking COPI vesicles to Golgi membranes. J Cell Biol. 1998; 140:1013–1021. [PubMed: 9490716]
32. Linstedt AD, Foguet M, Renz M, Seelig HP, Glick BS, Hauri HP. A C-terminally-anchored Golgi protein is inserted into the endoplasmic reticulum and then transported to the Golgi apparatus. Proc Natl Acad Sci U S A. 1995; 92:5102–5105. [PubMed: 7761455]
33. Jessop CE, Chakravarthi S, Garbi N, Hämmerling GJ, Lovell S, Bulleid NJ. ERp57 is essential for efficient folding of glycoproteins sharing common structural domains. EMBO J. 2007; 26:28–40. [PubMed: 17170699]
34. Pressinotti NC, Klocker H, Schäfer G, Luu VD, Ruschhaupt M, Kuner R, et al. Differential expression of apoptotic genes PDIA3 and MAP3K5 distinguishes between low- and high-risk prostate cancer. Mol Cancer. 2009; 8:130. [PubMed: 20035634]
35. Frenkel Z, Shenkman M, Kondratyev M, Lederkremer GZ. Separate roles and different routing of calnexin and ERp57 in endoplasmic reticulum quality control revealed by interactions with asialoglycoprotein receptor chains. Mol Biol Cell. 2004; 15:2133–2142. [PubMed: 14978212]
36. Bi S, Hong PW, Lee B, Baum LG. Galectin-9 binding to cell surface protein disulfide isomerase regulates the redox environment to enhance T-cell migration and HIV entry. Proc Natl Acad Sci U S A. 2011; 108:10650–10655. [PubMed: 21670307]
37. Miserey-Lenkei S, Chalancon G, Bardin S, Formstecher E, Goud B, Echard A. Rab and actomyosin-dependent fission of transport vesicles at the Golgi complex. Nat Cell Biol. 2010; 12:645–654. [PubMed: 20562865]
38. Rosing M, Ossendorf E, Rak A, Barnekow A. Giantin interacts with both the small GTPase Rab6 and Rab1. Exp Cell Res. 2007; 313:2318–2325. [PubMed: 17475246]
39. Tatebe H, Morigasaki S, Murayama S, Zeng CT, Shiozaki K. Rab-family GTPase regulates TOR complex 2 signaling in fission yeast. Curr Biol. 2010; 20:1975–1982. [PubMed: 21035342]
40. Del Nery E, Miserey-Lenkei S, Falguières T, Nizak C, Johannes L, Perez F, et al. Rab6A and Rab6A' GTPases play non-overlapping roles in membrane trafficking. Traffic. 2006; 7:394–407. [PubMed: 16536738]
41. Micaroni M, Stanley AC, Khromykh T, Venturato J, Wong CX, Lim JP, et al. Rab6a/a' are important Golgi regulators of pro-inflammatory TNF secretion in macrophages. PLoS One. 2013; 8(2):e57034. [PubMed: 23437303]
42. Obinata D, Takayama KI, Urano T, Murata T, Ikeda K, Horie-Inoue K, et al. ARFGAP3, an androgen target gene, promotes prostate cancer cell proliferation and migration. Int J Cancer. 2012; 130:2240–2248. [PubMed: 21647875]
43. Gerhardt J, Steinbrech C, Büchi O, Behnke S, Bohnert A, Fritzsche F, et al. The androgen-regulated Calcium-Activated Nucleotidase 1 (CANT1) is commonly overexpressed in prostate cancer and is tumor-biologically relevant in vitro. Am J Pathol. 2011; 178:1847–1860. [PubMed: 21435463]
44. Rokhlin OW, Taghiyev AF, Guseva NV, Glover RA, Chumakov PM, Kravchenko JE, et al. Androgen regulates apoptosis induced by TNFR family ligands via multiple signaling pathways in LNCaP. Oncogene. 2005; 24:6773–6784. [PubMed: 16007156]

45. Diao A, Frost L, Morohashi Y, Lowe M. Coordination of golgin tethering and SNARE assembly: GM130 binds syntaxin 5 in a p115-regulated manner. J Biol Chem. 2008; 283:6957–6967. [PubMed: 18167358]

46. Ruan Q, Wang Q, Xie S, Fang Y, Darzynkiewicz Z, Guan K, et al. Polo-like kinase 3 is Golgi localized and involved in regulating Golgi fragmentation during the cell cycle. Exp Cell Res. 2004; 294:51–59. [PubMed: 14980500]

47. True L, Coleman I, Hawley S, Huang CY, Gifford D, Coleman R, et al. A molecular correlate to the Gleason grading system for prostate adenocarcinoma. Proc Natl Acad Sci U S A. 2006; 103:10991–10996. [PubMed: 16829574]

48. Hagisawa S, Ohyama C, Takahashi T, Endoh M, Moriya T, Nakayama J, et al. Expression of core 2 beta1,6-N-acetylglucosaminyltransferase facilitates prostate cancer progression. Glycobiology. 2005; 15:1016–1024. [PubMed: 15932919]

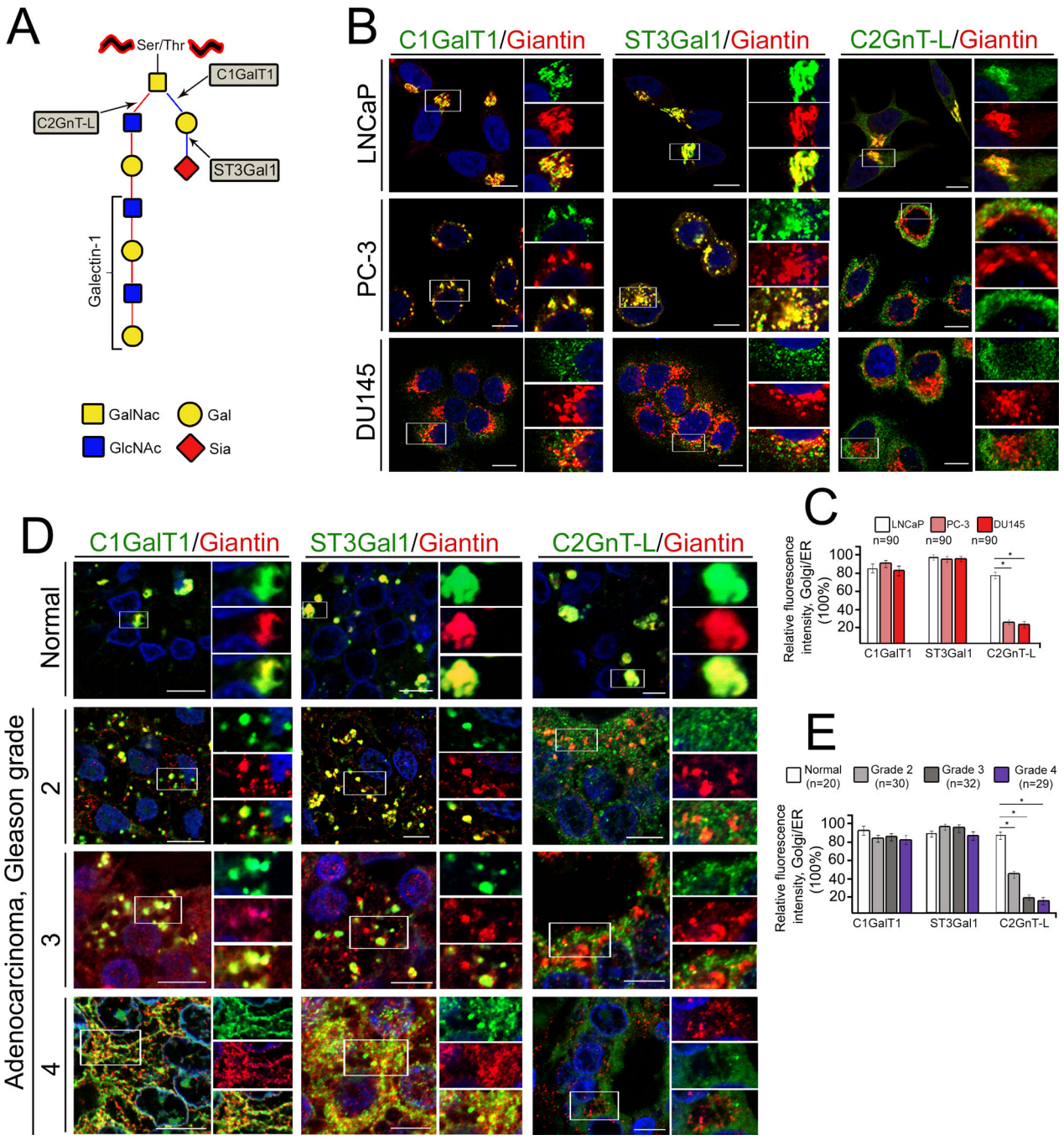

Figure 1. Altered Golgi morphology and differential distribution of C1GalT1 and ST3Gal1 versus C2GnT-L in prostate cancer cells and adenocarcinoma tumors

(A) Schema of selective mucin core 1 and core 2-associated O-glycans in mammalian cells. The core 1 O-glycan is generated by C1GalT1. ST3Gal1 and C2GnT-L compete for the core 1 substrate to generate Siaα2-3Galβ1-3GalNAc and Galβ1-3(GlcNAcβ1-6)GalNAc, respectively. GlcNAc can be extended by a polylactosamine (Gal-GlcNAc) sequence to render these cells susceptible to galectin-1-induced apoptosis. **(B–E)** Colocalization of GTs with giantin in LNCaP, PC-3 and DU145 cells, and in normal prostate tissues and different

grades of prostate adenocarcinoma. Quantification of relative fluorescence intensity of indicated GTs in ER vs. Golgi in B & D is shown in C &E, respectively. White boxes in each panel are enlarged and shown at the right side as green, red and merged images. All confocal images were acquired with same imaging parameters. Bars, 10 μm; *, $p<0.001$.

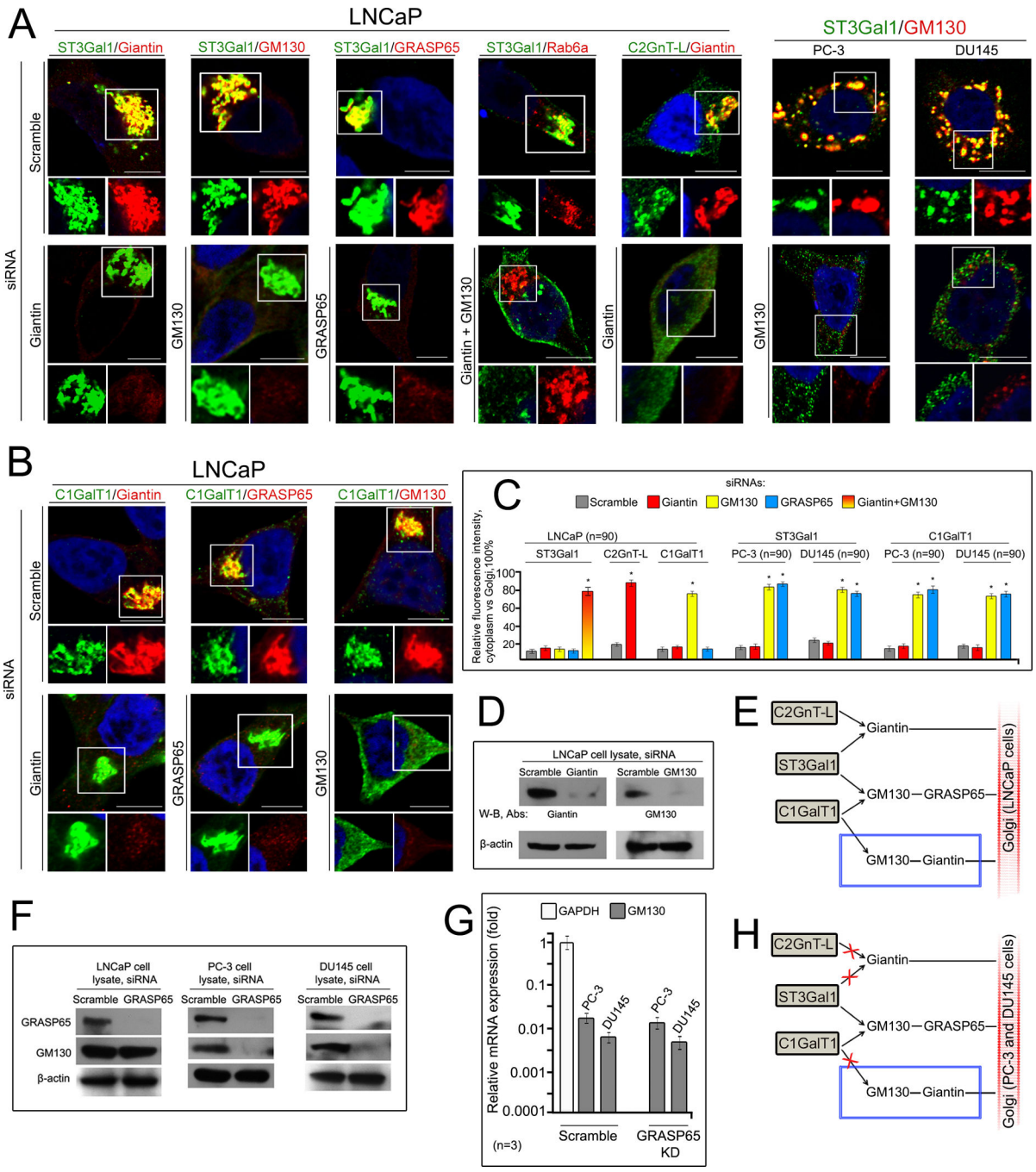

Figure 2. ST3Gal1 uses GM130-GRASP65 and giantin, and C2GnT-L utilizes giantin for Golgi targeting

(A, B) Colocalization images of ST3Gal1, C2GnT-L and C1GalT1 with Golgi markers in cells treated with golgin-specific siRNAs. The images inside the white boxes are enlarged and shown as green and red channels at the bottom of each panel. All confocal images were acquired with same imaging parameters; bars, 10 μm. **(C)** Quantification of the fluorescence intensity of cytoplasm/Golgi for indicated GTs in cells treated with golgin-specific siRNAs; *, p<0.001. **(D)** Giantin and GM130 W-B of the lysates of cells treated with scramble,

giantin, or GM130 siRNAs. **(E)** Schema showing Golgi docking sites for C1GalT1, ST3Gal1 and C2GnT-L in LNCaP cells. The highlighted blue box indicates alternate Golgi targeting site for C1GalT1 in the absence of GRASP65. **(F)** GRASP65 and GM130 W-B of the lysates of cells treated with scramble or GRASP65 siRNAs. **(G)** Quantitative real-time PCR analysis of the mRNA of GM130 gene in PC-3 and DU145 cells treated with scramble or GRASP65 siRNAs. The gene expression levels were calculated by the ΔCt method as described in Materials and Methods and expressed as the relative amount to that of GAPDH(100 %). **(H)** Schema showing the Golgi targeting sites for C1GalT1 and ST3Gal1 in PC-3 and DU145 cells.

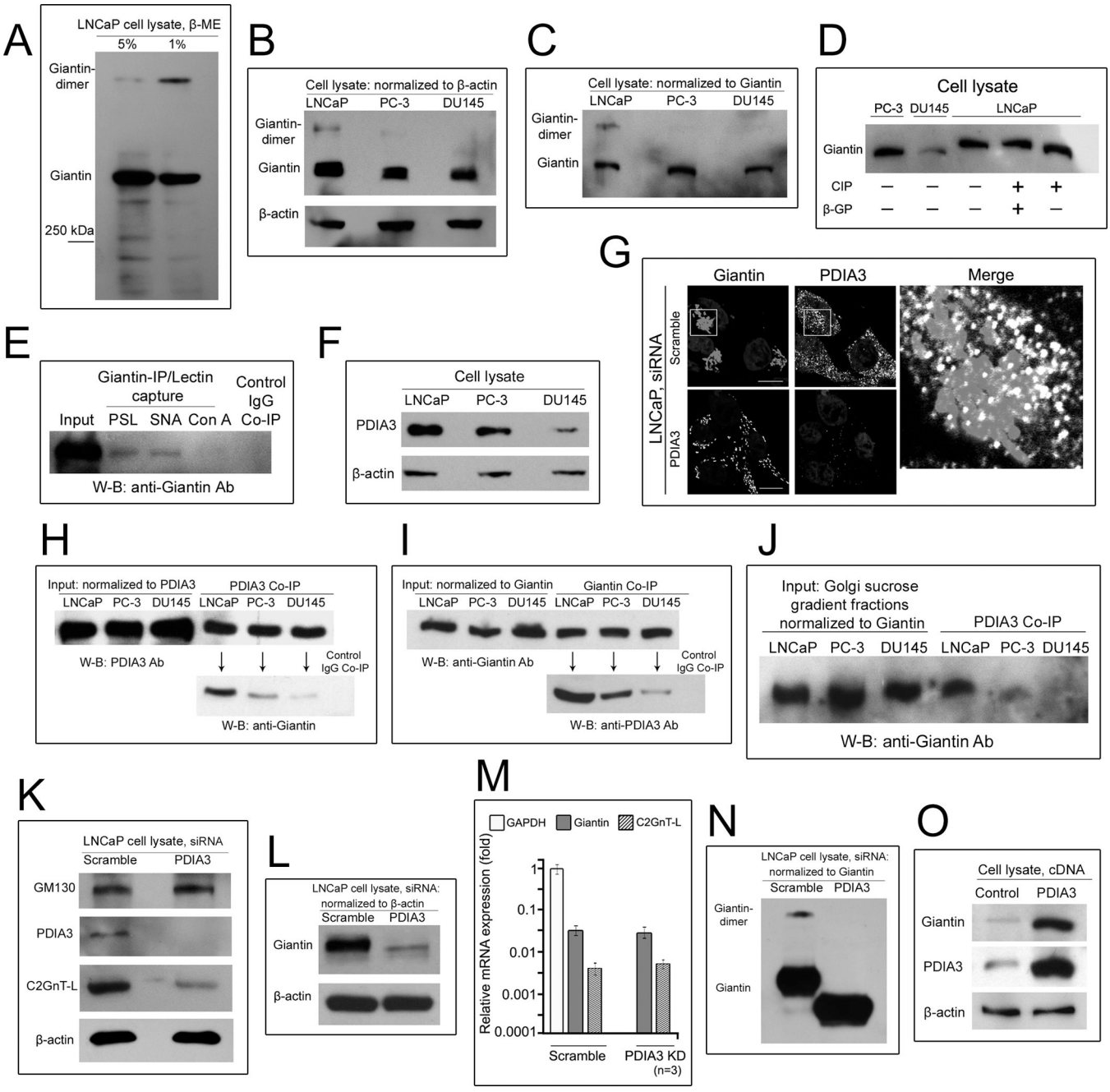

Figure 3. Giantin is a phosphorylated homo-dimer in LNCaP cells

(A) Giantin W-B of LNCaP cell lysates prepared under high (5%) and low (1%) concentrations of β-mercaptoethanol (ME). **(B, C)** Giantin W-B of the cell lysates prepared under low ME. Samples were normalized to either β-actin or giantin. **(D)** Band-shift assay of phosphorylated giantin. The lysates of LNCaP cells were treated with CIP in the presence or absence of β-GP. **(E)** LNCaP cell lysate was subjected to immunoprecipitation with giantin Ab followed by pull-down using PSL, SNA, or Con A lectin. Giantin W-B of these samples shows that giantin is a glycoprotein with complex-type N-glycans. **(F)** PDIA3 W-B of the lysates of LNCaP, PC-3 and DU145 cells. **(G)** Images of giantin and PDIA3 in LNCaP cells

treated with scramble or PDIA3 siRNAs. The Golgi area in the white box is enlarged and displayed as merged grey (giantin) and white (PDIA3) colors at the right side. **(H, I)** PDIA3 and giantin W-B of the complexes pulled down with anti-giantin and anti-PDIA3 Abs from cell lysates adjusted to equal amounts of PDIA3 (H) and giantin (I), respectively. **(J)** Giantin W-B of the complexes pulled down withanti-PDIA3 Ab from the Golgi fractions adjusted to equal amounts of giantin. **(K, L)** GM130, PDIA3, C2GnT-L and giantin W-B of the lysates of LNCaP cells treated with scramble or PDIA3 siRNAs and normalized to β-actin. **(M)** Quantitative real-time PCR analysis of the mRNA of giantin and C2GnT-L genes in LNCaP cells treated with scramble or PDIA3 siRNAs. **(N)** Giantin W-B of the lysates of LNCaP cells treated with scramble or PDIA3 siRNAs and normalized to giantin. **(O)** Giantin W-B of the lysates of LNCaP cells transfected with or without a full length PDIA3 cDNA. All SDS PAGE was performed with 6 or 8% gel.

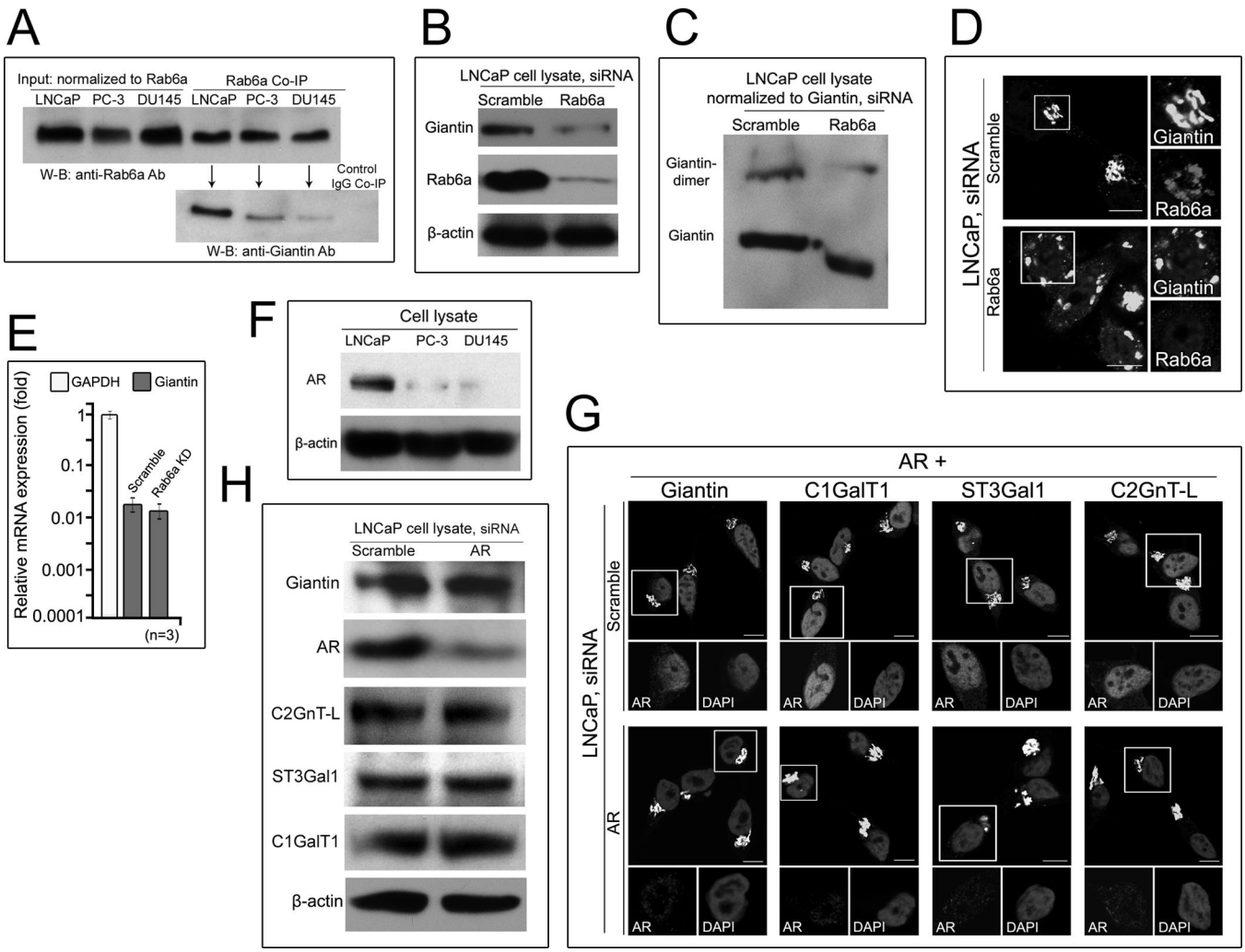

Figure 4. Rab6a regulates dimerization and phosphorylation of giantin

(A) Giantin and Rab6a W-B of the complexes pulled down with anti-Rab6a Ab from the lysates of cells adjusted to equal amounts of Rab6a. **(B, C)** Rab6a and giantin W-B of the lysates of LNCaP cells treated with scramble or Rab6a siRNAs. Samples were normalized to either β-actin (B) or giantin (C). All SDS PAGE was performed with 6 or 8% gel. **(D)** Knockdown of Rab6a causes Golgi fragmentation. Images of giantin and Rab6a in LNCaP cells treated with scramble or Rab6a siRNAs. The Golgi area in the white boxes is enlarged and displayed as giantin or Rab6a channels on the right side of each panel. **(E)** Quantitative real-time PCR analysis of the mRNA of giantin gene in LNCaP cells treated with scramble or Rab6a siRNAs. **(F)** AR W-B of the lysates of LNCaP, PC-3 and DU145 cells normalized to β-actin. **(G)** Images of AR co-staining with giantin, C1GalT1, ST3Gal1 and C2GnT-L in LNCaP cells treated with scramble or AR siRNAs. The images inside the white boxes are enlarged and shown as AR and DAPI (nucleus) channels at the bottom of each panel. All confocal images were acquired with same imaging parameters; bars, 10 μm. **(H)** Giantin, AR, C2GnT-L, ST3Gal1, and C1GalT1 W-B of the lysates of LNCaP cells treated with scramble or AR siRNAs and normalized to β-actin.

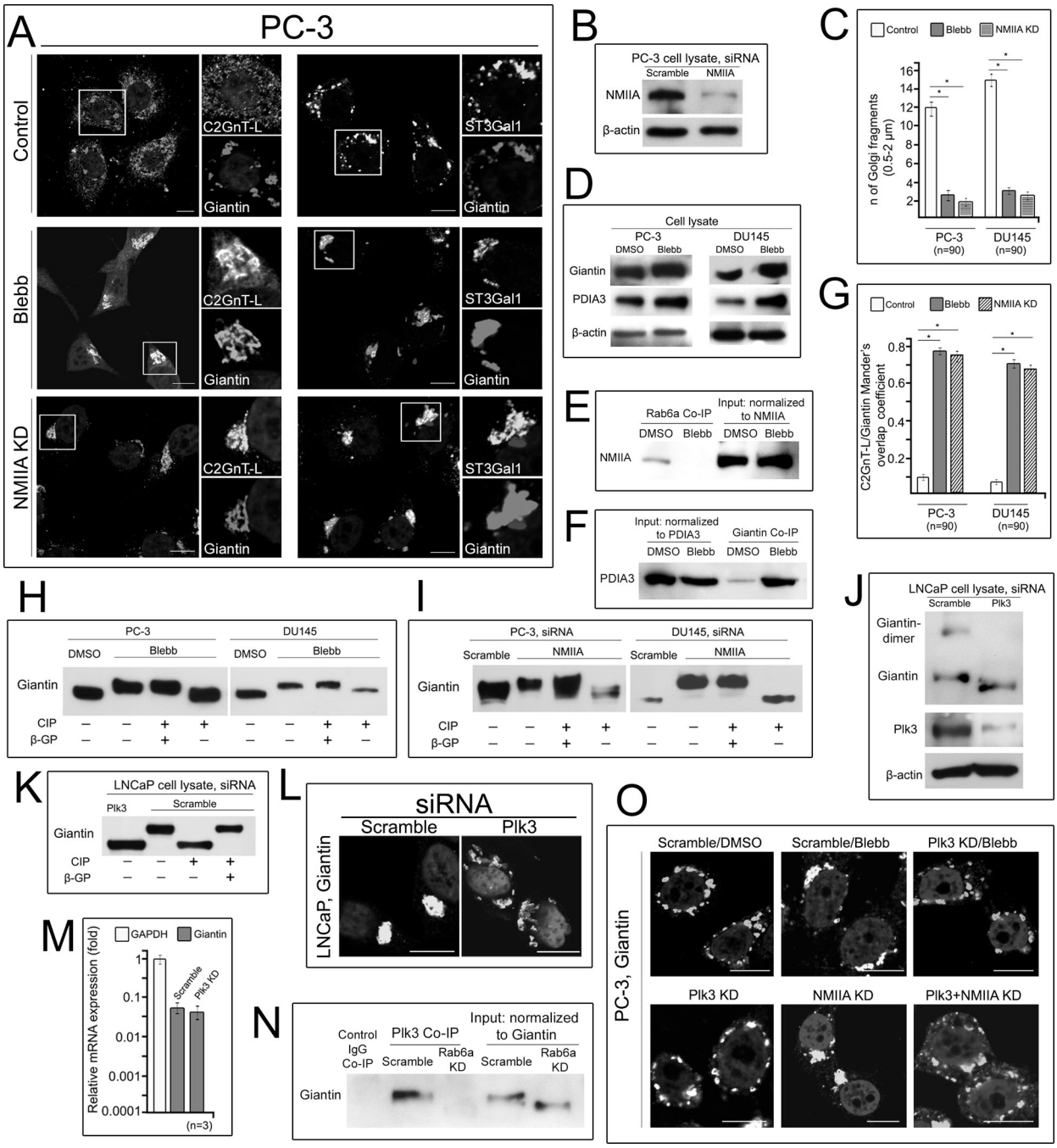

Figure 5. Inhibition or knockdown of NMIIA in PC-3 and DU145 cells induces dimerization of giantin, and restores compact Golgi and C2GnT-L intra-Golgi localization

(A) Colocalization of C2GnT-L and ST3Gal1 with giantin in PC-3 cells treated with DMSO, Blebbistatin or NMIIA siRNAs. **(B)** NMIIA W-B of the lysate of PC-3 cells after NMIIA KD. **(C)** Quantification of Golgi fragments (0.5 to 2 μm in size) in the cells shown in A; *, p<0.001. **(D)** Giantin and PDIA3 W-B of the lysates of cells after Blebbistatin treatment. **(E, F)** NMIIA and PDIA3 W-B of the complexes pulled down with Rab6a and giantin Abs, respectively, from the lysates of PC-3 cells treated with DMSO or Blebbistatin. **(G)**

Quantification of Mander's coefficient of C2GnT-L and giantin colocalization of cells presented in A; *, $p<0.001$. (**H, I)** The lysates of cells pretreated with Blebbistatin or NMIIA siRNAs were incubated with CIP with or without β-GP. **(J, K)** Giantin W-B of the lysates of LNCaP cells treated with scramble or Plk3 siRNAs. The control lysates were incubated with CIP with or without β-GP. **(L)** Images of giantin in LNCaP cells treated with scramble or Plk3 siRNAs. **(M)** Quantitative real-time PCR analysis of the mRNA of giantin gene in LNCaP cells treated with scramble or Plk3 siRNAs. **(N)** Giantin W-B of the complexes pulled down with anti-Plk3 Ab from lysates of LNCaP cells treated with scramble or Rab6a Abs, adjusted to equal amounts of giantin. **(O)** Images of giantin in PC-3 cells treated with scramble and Plk3 siRNAs followed by Blebbistatin, or Plk3, NMIIA and NMIIA plus Plk3 siRNAs. Bars, 10 μm. Gradient gel (4–12%) for G, H and J, and 6 or 8% gel for the rest were used.

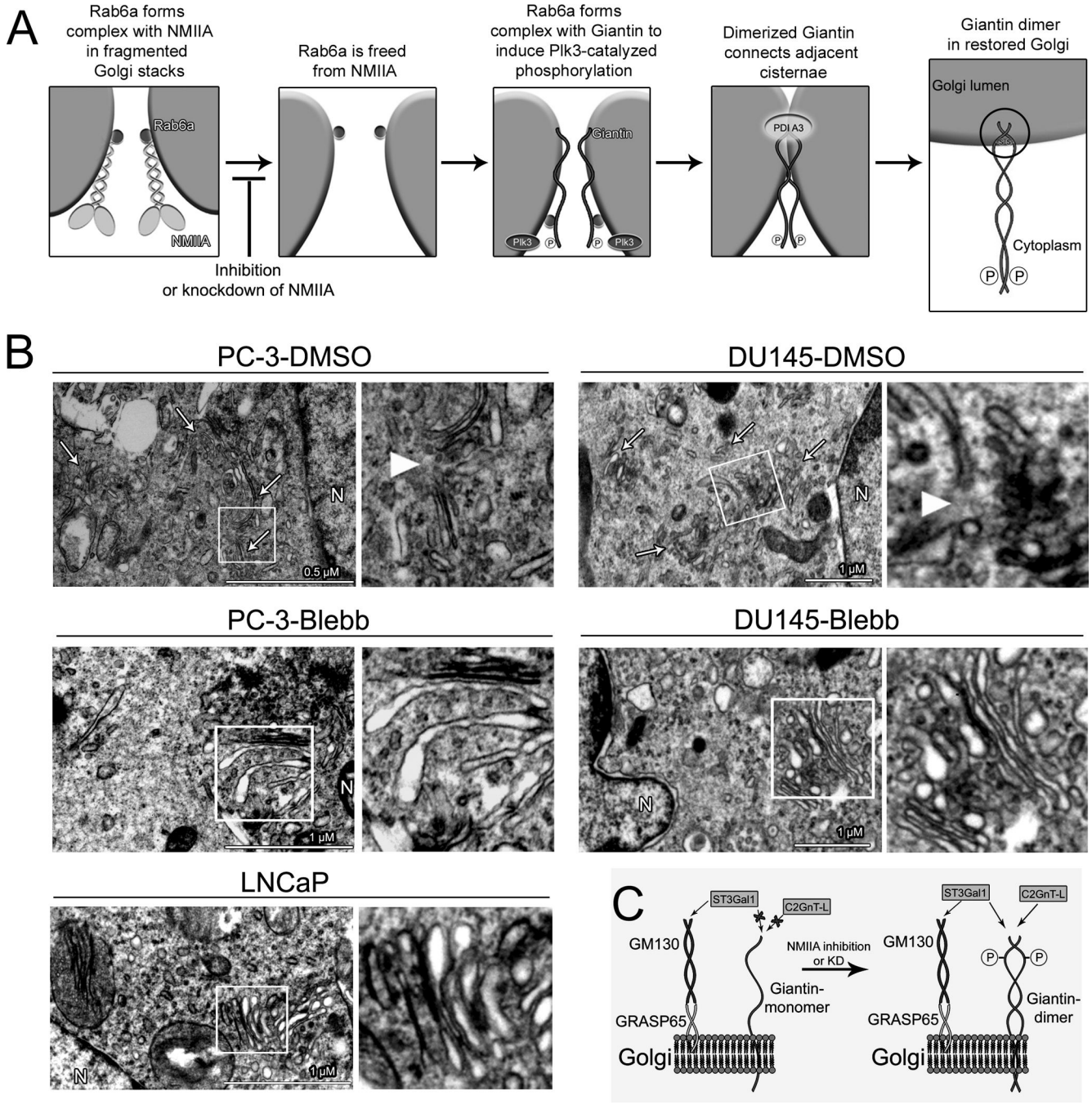

Figure 6. The proposed model of NMIIA inhibition or knockdown-induced formation of giantin dimer and restoration of compact Golgi morphology in androgen-refractory prostate cancer cells

(A) Inhibition or KD of NMIIA frees up Rab6a to interact with and induce Plk3-catalyzed phosphorylation of giantin. Rab6a connects two adjacent Golgi cisternae by forming complex with a giantin monomer presumably via the N-terminal region of giantin (aa 253–357) (38). With the assistance of PDIA3, phosphorylated giantin is dimerized via its C-terminal (28, 32) followed by coiled-coil association, which further stabilizes the giantin structure. **(B)** Transmission electron microscopic images of LNCaP cells as well as PC-3

and DU145 cells treated with DMSO or Blebbistatin. In PC-3 and DU145 cells treated with DMSO, Golgi fragments are distributed in the perinuclear region as well as cytoplasm (white arrows), and gaps (white arrowhead) are found between Golgi stacks. In both cells, Blebbistatin treatment leads to the appearance of the Golgi morphology phenotypically close to that in LNCaP cells. N, nucleus. **(C)** Schema showing the correction of the defective phosphorylation and dimerization of giantin as well as Golgi targeting of C2GnT-L in PC-3 and DU145 cells by inhibition or KD of NMIIA.

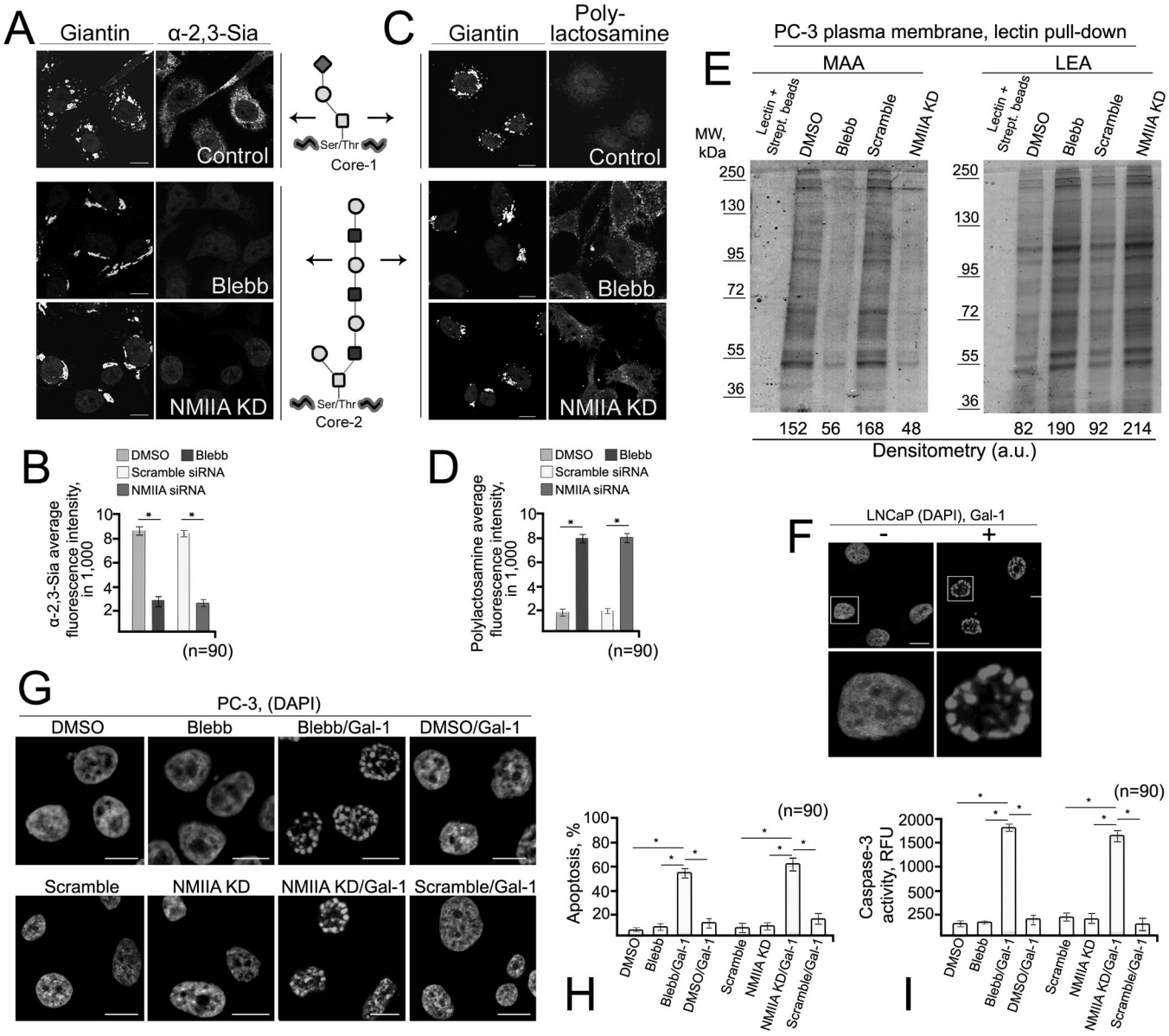

Figure 7. Restoration of the compact Golgi in PC-3 and DU145 cells redirects O-glycosylation pathway

(A, C) Images of immunostained giantin, MAA lectin-stained α-2,3-Sia and LEA lectin-stained polylactosamine in PC-3 cells treated with Blebbistatin or NMIIA siRNAs. **(B, D)** Quantification of α-2,3-Sia and polylactosamine-specific average integrated fluorescence (in a.u.) in the cells shown in A and C, respectively. **(E)** The 8% SDS PAGE of PC-3 cell plasma membrane fraction pull-down with biotinylated lectin MAA or LEA followed by capturing with streptavidin magnet beads. **(F)** DAPI staining of LNCaP cells treated with 10 μM galectin-1 for 7 h. Cells treated with corresponding amount of DTT served as a control. **(G)** DAPI staining of PC-3 cells treated with DMSO, Blebbistatin, or scramble or NMIIA siRNAs and then with or without 10 μM galectin-1. **(H, I)** The percentage of apoptotic cells and caspase-3 activity in cells presented in G. Apoptotic nuclei were counted in 30 different fields, each from three independent experiments and the apoptotic cells were expressed as %

of total cells. Caspase-3 activity is expressed as mean relative fluorescence units (RFU) from three independent experiments. Bars, 10 μm; *, $p<0.001$.